JPE 18-1-14

https://doi.org/10.6113/JPE.2018.18.1.147
ISSN(Print): 1598-2092 / ISSN(Online): 2093-4718

Incremental Passivity Based Control for DC-DC Boost Converters under Time-Varying Disturbances via a Generalized Proportional Integral Observer

Wei He*, Shihua Li†, Jun Yang*, and Zuo Wang*

*,†Key Laboratory of Measurement and Control of CSE, Ministry of Education, School of Automation, Southeast University, Nanjing, China

Abstract

In this paper, the voltage tracking control of a conventional DC-DC boost converter affected by unknown, time-varying circuit parameter perturbations is investigated. Based on the fundamental property of incremental passivity, a passivity based control law is designed. Then, to obtain a better disturbance rejection property, two generalized proportional integral (GPI) observers are employed to estimate the time-varying uncertainties in the output voltage and inductor current channels, and the estimated values are applied as feedforward compensation. Moreover, the global trajectory tracking performance of a system with disturbances is ensured under the composite controller. Finally, simulation and experiment studies are provided to demonstrate the feasibility and effectiveness of the proposed method. The results show that the proposed controller delivers a promising disturbance rejection capability as well as a good nominal tracking performance.

Key words: DC-DC boost converter, Disturbance, Generalized Proportional Integral (GPI) observer, Passivity-Based Control (PBC)

I. INTRODUCTION

DC-DC power converters have been extensively employed in industrial applications, such as renewable energy sources (solar photovoltaic, wind turbine, etc.), electrical vehicles, adjustable-speed drives and welding machines [1]-[3]. The boost type converter, also known as a step-up converter, is applied in applications where the required output voltage is higher than the input voltage [20]. It is noticed that the circuit naturally behaves as a nonlinear and time-varying system due to its switching operation. In addition, its average model is a bilinear system. In other words, the model of the boost converter has a bilinear term which is the product of the duty ratio and the states. In addition, the boost converter also exhibits the non-minimum phase phenomenon with respect to the output to be controlled. Furthermore, the control performance of this circuit is often seriously influenced by various circuit parameter uncertainties, such as load resistance variations and input voltage changes [35], [36], [39]. Therefore, a feasible and efficient controller design for the DC-DC boost converter brings great challenges to academic and industrial practitioners [4]-[8].

The controller of a DC-DC converter aims to regulate the output voltage around the reference value without a steady-state error. Moreover, the closed-loop system should be robustness against various uncertainties for reliable operating conditions [12].

Over the past decades, many elegant control strategies, such as, backstepping control [9], input/output feedback linearization [14], robust control [11], [12], LMI based control [10], sliding mode control [13], [16], predictive control [18], optimal control [17], Lyapunov-based control [21] and fuzzy logic control [19], have been widely investigated in the literature for DC-DC power converters. These methods effectively enhance control performances in different spheres.

Passivity-based control (PBC) is one of the most practical control techniques. It has been successfully applied in industrial applications, such as mechanical systems, power systems, electromechanical systems, underwater vehicles and process

Manuscript received Aug. 1, 2016; accepted Sep. 7, 2017
Recommended for publication by Associate Editor Sung-Jin Choi.
†Corresponding Author: lsh@seu.edu.cn
Tel: +86-25-83793785, Southeast University
*Key Laboratory of Measurement and Control of CSE, Ministry of Education, School of Automation, Southeast University, China

control [5], [25], [27]. This control method was first proposed in [23], where the term PBC was coined to design a simple controller to render a closed loop system passive with a storage function. It should be noted that this storage function to be assigned should have an isolated minimum at a given equilibrium point and can be usually qualified as a Lyapunov function for the stability analysis [26]. When compared to other nonlinear control methods, the PBC is simple, effective and easily implemented. In addition, the physical property of its control action can be clearly given [24].

The parallel-damped PBC (PD-PBC) method presented in [30] obtained remarkable performances. The main merits of the parallel damping approach over the series damping injection lies in that it is insensitive to load variations and output feedback is achieved. However, the stability result involved is locally asymptotic stability. In [34], to eliminate the steady state error raised by parameter uncertainties, a composite controller is proposed by a combination of the PD-PBC and the conventional PID. The sufficient condition for the asymptotic stability of an augmented system is presented by applying a Jacobian linearization model. However, the linearization of nonlinear non-minimum phase systems may give rise to poor performances under different operating points and large disturbances. The authors of [32] introduced a simple feedback control law based on the passivity property to achieve tracking of the trajectory for a class of bilinear systems. Moreover, the stability result is global and holds for the positive gain of the controller as long as the rank condition is achieved. It is pointed out that the methods mentioned above [32], [34] counteract the undesirable effects of disturbances and uncertainties by integral action. Nevertheless, it is well known that integral action is able to eliminate the effects caused by a constant disturbance and results in a steady-state error in the presence of time-varying disturbances. Therefore, an adaptive scheme is utilized in [37] to effectively estimate the time-varying load resistance in power converters.

As a practical alternative approach, the generalized proportional integral (GPI) observer used in this study, has been shown to be effective in estimating time-varying disturbances including parameter uncertainties, external disturbances as well as un-modeled dynamics [31], [38]. The main merit of the GPI observer lies in the fact that it is simple and easy to implement since this observer is based on a linear configuration. There are many applications using GPI observer such as robots [29], underactuated mobile manipulators [33], PMSM servo systems [15], [22] and so on.

In this paper, taking into account the natural nonlinear characters of DC-DC boost converter systems and aiming to improve control performance, a composite control method, called PBC+GPIO, is proposed to achieve stability and robustness in the presence of time-varying disturbances including load resistance changes, input voltage variations, inductance and capacitance parameter perturbations, and parasitic resistance. The feedback part design is based on the passivity property borrowed from [32]. The main contributions here are presented as follows. (1) The generalized proportional integral (GPI) observers and the corresponding feed-forward parts are introduced to form a composite PBC+GPIO controller. (2) The global asymptotic stability of a DC-DC boost converter system is strictly guaranteed in the presence of time-varying disturbances on the basis of the passivity theory and input to state stable (ISS) property. The anti-disturbance performance of the DC-DC boost converter is obviously enhanced. Finally, the effectiveness of the proposed method is shown by the simulation and experimental results.

The rest of paper is organized as follows. Section II presents an average model of DC-DC boost converter systems. Section III gives a detailed design of the passivity-based controller with GPI observers and a stability analysis of the entire closed-loop system. Section IV describes simulation and experimental results for evaluating the effectiveness of the proposed control method. Section V presents some conclusions.

II. Model Description and Problem Formulation

A. Model Description of a DC-DC Boost Converter

A typical PWM based DC-DC boost power converter structure is shown in Fig. 1, where i_L is the inductance current, v_o is the average output capacitor voltage, V_d is the reference output voltage, L is the circuit inductance, C is the circuit capacitor, R is the circuit load resistance, r_L, r_C is the circuit parasitic resistance, E is the voltage of the external source, and $\mu \in [0,1]$ is the duty ratio function taken as the control signal of the PWM. The converter dynamic model is described as follows.

When the switch is on:

$$\begin{cases} L\dot{i}_L = -r_L i_L + E, \\ C\dot{v}_o = -\dfrac{v_o}{R + r_c}. \end{cases}$$

When the switch is off:

$$\begin{cases} L\dot{i}_L = -r_L i_L - \dfrac{r_c R}{R + r_c} i_L - (1 + \dfrac{r_c}{R + r_c}) v_o + E, \\ C\dot{v}_o = \dfrac{R}{R + r_c} i_L - \dfrac{v_o}{R + r_c}. \end{cases}$$

The dynamic model of such a generic DC-DC boost converter can be obtained and given by:

$$\begin{cases} \dot{i}_L = -\dfrac{r_L}{L} i_L - (1-\mu)\dfrac{r_c R}{L(R + r_c)} i_L - (1-\mu)(1 + \dfrac{r_c}{R + r_c})\dfrac{v_o}{L} + \dfrac{E}{L}, \\ \dot{v}_o = (1-\mu)\dfrac{R i_L}{C(R + r_c)} - \dfrac{v_o}{C(R + r_c)}. \end{cases} \quad (1)$$

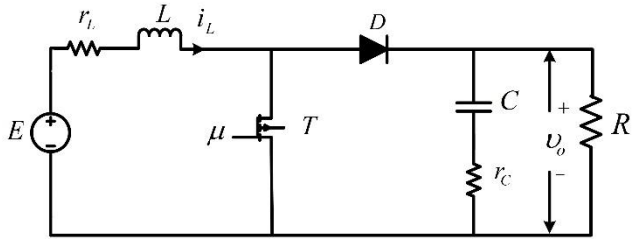

(a)

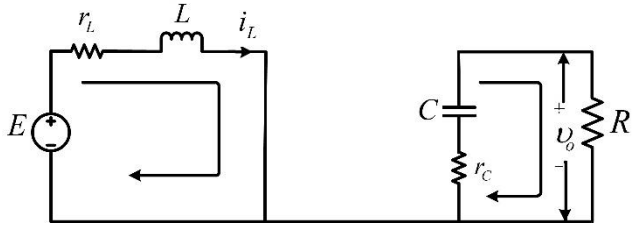

(b)

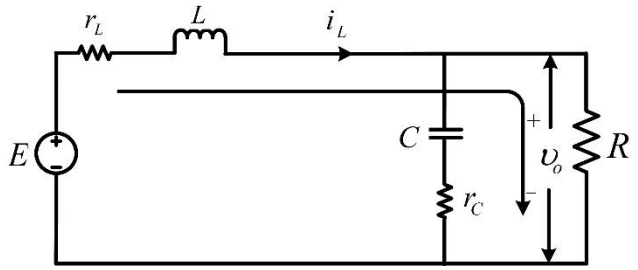

(c)

Fig. 1. Circuit diagram of a DC-DC boost converter: (a) circuit configuration; (b) a switch ON case; (c) a switch OFF case.

B. Problem Formulation

Considering the various uncertainties in a DC-DC boost converter, the dynamic model (1) can be given as follows:

$$\begin{cases} \dot{i}_L = a_1(1-\mu)v_o + b + d_1, \\ \dot{v}_o = a_2(1-\mu)i_L + a_3 v_o + d_2, \end{cases} \tag{2}$$

where d_1 and d_2 are the lumped time-varying disturbances that are expressed as:

$$\begin{cases} d_1 = \delta_1 i_L + \delta_2(1-\mu)v_o + \delta_b, d_2 = \delta_3 v_o + \delta_4(1-\mu)i_L, \\ a_1 = -\dfrac{1}{L_0}, a_2 = \dfrac{1}{C_0}, a_3 = -\dfrac{1}{R_0 C_0}, b = \dfrac{E_0}{L_0}, \\ \delta_1 = -\dfrac{r_L}{L} - (1-\mu)\dfrac{r_c R}{R+r_c}, \delta_2 = \dfrac{1}{L_0} - \dfrac{1}{L}(1+\dfrac{r_c}{R+r_c}), \\ \delta_3 = \dfrac{1}{R_0 C_0} - \dfrac{1}{C(R+r_c)}, \delta_4 = -\dfrac{1}{C_0} + \dfrac{R}{C(R+r_c)}, \delta_b = -\dfrac{E_0}{L_0} + \dfrac{E}{L}, \end{cases}$$

and R_0, C_0, L_0 and E_0 are the nominal values of the parameters R, C, L and E, respectively.

Defining $x = \begin{bmatrix} i_L & v_o \end{bmatrix}^T$ and $u = 1-\mu$, system (2) can be written as:

$$\dot{x} = Ax + uBx + \eta + d, \tag{3}$$

where:

$$A = \begin{bmatrix} 0 & 0 \\ 0 & a_3 \end{bmatrix}, \quad B = \begin{bmatrix} 0 & a_1 \\ a_2 & 0 \end{bmatrix},$$

$$\eta = \begin{bmatrix} b & 0 \end{bmatrix}^T, \quad d = \begin{bmatrix} d_1 & d_2 \end{bmatrix}^T.$$

For system (3), it is easy to find a positive-definite symmetric matrix P with this form:

$$P = \begin{bmatrix} L_0 & 0 \\ 0 & C_0 \end{bmatrix},$$

such that:

$$PA + A^T P \le 0, PB + B^T P = 0. \tag{4}$$

To simplify the notation, define the following:

$$Q = -\frac{1}{2}(PA + A^T P).$$

Therefore, it is natural to recast the control problem for a DC-DC boost converter in terms of designing a suitable controller so that stability and robustness can be achieved in the presence of time-varying disturbances. More precisely, the global tracking control problem is to find a dynamic state feedback controller with the form:

$$u = H(x, x_*, u_*), \tag{5}$$

so that:

$$\lim_{t\to\infty}[x(t) - x_*(t)] = 0$$

for all of the initial conditions $x(0)$, time-varying disturbances and admissible trajectories x_*.

III. Global Tracking Controller Design

This section concentrates on the disturbance rejection problem of DC-DC boost converter systems. The control structure of a DC-DC boost converter system is designed as shown in Fig. 2. A composite controller is proposed by the following two steps. First, based on passivity theory, a feedback controller is designed for DC-DC boost converters. Second, two GPI observers are introduced to estimate the uncertainties in the output voltage and inductor current channels, respectively.

A. Generalized Proportional Integral Observer Design

As previously mentioned, the disturbances are unmeasurable time-varying signals. Thus, the corresponding feedforward control design is considered to reasonably compensate them.

Suppose that the time-varying disturbances d_1 and d_2 in system (3) and a finite number of its derivatives $d_1^{(j)}$ and $d_2^{(k)}$ are uniformly absolutely bounded, where $j=1,2,\cdots,m$ and $k=1,2,\cdots,p$ for some large integers m and p. Defining $z_0 = d_1$, $z_1 = \dot{d}_1, \cdots, z_m = d_1^{(m)}$, $\eta_0 = d_2$, $\eta_1 = \dot{d}_2, \cdots, \eta_p = d_2^{(p)}$, based on the flatness output i_L, v_o for system (2), two GPI observers are designed as:

$$GPIO\ I:\begin{cases}\dot{\hat{i}}_L = a_1(1-\mu)v_o + b + \hat{z}_0 + \lambda_{1m}(i_L - \hat{i}_L),\\ \dot{\hat{z}}_0 = \hat{z}_1 + \lambda_{1(m-1)}(i_L - \hat{i}_L),\\ \dot{\hat{z}}_1 = \hat{z}_2 + \lambda_{1(m-2)}(i_L - \hat{i}_L),\\ \quad\vdots\\ \dot{\hat{z}}_{m-1} = \lambda_{10}(i_L - \hat{i}_L),\end{cases} \tag{6}$$

$$GPIO\ II:\begin{cases}\dot{\hat{v}}_o = a_2(1-\mu)i_L + a_3\hat{v}_o + \hat{\eta}_0 + \lambda_{2p}(v_o - \hat{v}_o),\\ \dot{\hat{\eta}}_0 = \hat{\eta}_1 + \lambda_{2(p-1)}(v_o - \hat{v}_o),\\ \dot{\hat{\eta}}_1 = \hat{\eta}_2 + \lambda_{2(p-2)}(v_o - \hat{v}_o),\\ \quad\vdots\\ \dot{\hat{\eta}}_{p-1} = \lambda_{20}(v_o - \hat{v}_o),\end{cases} \tag{7}$$

where $\hat{i}_L, \hat{z}_0, \hat{z}_1, \cdots, \hat{z}_{m-1}$ are the estimations of $i_L, d_1, \dot{d}_1, \cdots, d_1^{(m-1)}$, respectively, $\hat{v}_o, \hat{\eta}_0, \hat{\eta}_1, \cdots, \hat{\eta}_{p-1}$ are the estimations of $v_o, d_2, \dot{d}_2, \cdots, d_2^{p-1}$, respectively, λ_{1i}=*diag*(λ_{1i}^1, $\lambda_{1i}^2, \cdots, \lambda_{1i}^n$), $\lambda_{1i}^1, \lambda_{1i}^2, \cdots, \lambda_{1i}^n$ >0, (i=0,1,$\cdots$, m) and λ_{2j} =*diag*($\lambda_{2j}^1, \lambda_{2j}^2, \cdots, \lambda_{2j}^n$), $\lambda_{2j}^1, \lambda_{2j}^2, \cdots, \lambda_{2j}^n$ >0, (j=0,1,$\cdots$, p) are the coefficients of *GPIO I* and *II*, respectively, which are chosen so that the roots of the characteristic polynomial $p_{o1}(s)$ =[$P_{o1}^1(s), P_{o1}^2(s), \cdots, P_{o1}^n(s)$]^T and $p_{o2}(s)$ =[$P_{o2}^1, P_{o2}^2, \cdots, P_{o2}^n$]^T in the complex variable s:

$$\begin{aligned} p_{o1}(s) &= s^{(m+1)} + \lambda_{1m}s^m + \cdots + \lambda_{11}s + \lambda_{10},\\ p_{o2}(s) &= s^{(p+1)} + \eta_{2p}s^p + \cdots + \eta_{21}s + \eta_{20}\end{aligned} \tag{8}$$

are located in the left-half side of the complex plane. According to the analysis in [33], the time-varying disturbance estimation errors $e_{zi} = d_1^{(i)} - z_i, (i = 0,1,\cdots,m-1)$ and $e_{\eta i} = d_2^{(j)} - \eta_j, (j = 0,1,\cdots,p-1)$ can converge to their equilibrium points asymptotically.

Based on the GPI observers, the reference dynamics of system (3) are defined as follows:

$$\dot{x}_* = Ax_* + u_*Bx_* + b + \hat{d}, \tag{9}$$

where $x_* = \begin{pmatrix} x_{1*} & x_{2*}\end{pmatrix}^T$, $\hat{d} = \begin{pmatrix}\hat{d}_1 & \hat{d}_2\end{pmatrix}^T$.

It can be known that x_{2*} represents a desired output voltage V_d. According to (9), the desired reference values x_{1*} and u_* in this case can be obtained as:

$$x_{1*} = \frac{x_{2*}^2}{E_0 + \hat{d}_1}\left(\frac{1}{R_0} - \frac{C_0\hat{d}_2}{x_{2*}}\right), \quad u_* = \frac{E_0 + L_0\hat{d}_1}{x_{2*}}.$$

B. Passivity of an Incremental Nonlinear System

Taking into account system (3) and the reference trajectory (9) in the absence of disturbances, the error signals are defined as:

$$\tilde{x} = \begin{bmatrix} x_1 - x_{1*}\\ x_2 - x_{2*}\end{bmatrix} = \begin{bmatrix}\tilde{x}_1\\ \tilde{x}_2\end{bmatrix}, \quad \tilde{u} = u - u_*$$

and the output function is expressed as:

$$\tilde{y} = C(x_*)\tilde{x}, \tag{10}$$

where the map is defined as:

$$C(x_*) = x_*^T B^T P.$$

Lemma 1 [32]: Consider a storage function with the following form:

$$V(\tilde{x}) = \frac{1}{2}\tilde{x}^T P\tilde{x}, \tag{11}$$

the incremental passivity inequality holds for (11), that is:

$$\dot{V}(\tilde{x}) \le \tilde{y}^T\tilde{u}.$$

C. Controller Design

Definition 1 [28]: A continuous function $\alpha:[0,\alpha)\to[0,\infty)$ is said to belong to class κ if it is strictly increasing and $\alpha(0)$=0. A continuous function $\beta:[0,\alpha)\times[0,\infty)\to[0,\infty)$ is said to belong to class $\kappa\iota$ if, for each fixed s, the mapping $\beta(r, s)$ belongs to class κ with respect to r, for each fixed r, the mapping $\beta(r, s)$ is decreasing with respect to s, and $\beta(r,s)\to 0$ as $s\to 0$.

To introduce the notation of input-to-state stability (ISS), consider the system:

$$\dot{x} = f(t,x,u), x\in R^n, u\in R^m. \tag{12}$$

Definition 2 [28]: System (12) is said to have ISS if there exists a class $\kappa\iota$ function β and a class κ function γ so that for any initial state $x(t_0)$ and any bounded input $u(t)$, the solution $x(t)$ exists for all $t > t_0$ and satisfies:

$$\|x(t)\| \le \beta(\|x(t_0)\|, t - t_0) + \gamma(\sup_{t_0\le\tau\le t}\|u(t)\|),$$

such a function γ is referred to as an ISS-gain for system (12). The ISS implies that system (12) is bounded-input bounded-state stable when $u\neq 0$ and its zero solution is globally asymptotically stable.

Lemma 2 [28]: Consider a nonlinear system $\dot{x} = F(x,\omega)$ which is input-to-state stable (ISS). If the input satisfies $\lim_{t\to\infty}\omega(t) = 0$, then the states satisfy $\lim_{t\to\infty}x(t) = 0$.

The corresponding passive output is expressed as:

$\tilde{y} = x_*^T B^T P\tilde{x} = x_{1*}\tilde{x}_2 - x_{2*}\tilde{x}_1$.

Proposition 1: Consider DC-DC boost system (3) under the controller:

$$u = -k\tilde{y} + \frac{E_0 + \hat{d}_1}{x_{2*}}. \tag{13}$$

The global tracking of the trajectory is guaranteed, that is:

$$\lim_{t\to\infty}x(t) = x_*(t). \tag{14}$$

Proof: The error dynamics are obtained from the difference between (3) and (9). They are written as:

$$\dot{\tilde{x}} = (A + uB)\tilde{x} + \tilde{u}Bx_* - e_d, \tag{15}$$

where $e_d = \begin{pmatrix} e_{d_1} & e_{d_2} \end{pmatrix}^T, e_{d_1} = d_1 - \hat{d}_1, e_{d_2} = d_2 - \hat{d}_2$.

Consider the following Lyapunov candidate function:

$$W(\tilde{x}) = \frac{1}{2}\tilde{x}^T P\tilde{x}.$$

The time derivative of such function along the trajectory of system (15) is given by:

$$\begin{aligned} \dot{W} &= \tilde{x}^T P[(A+uB)\tilde{x} + \tilde{u}Bx_* - e_d] \\ &= -\tilde{x}^T Q\tilde{x} + \frac{1}{2}u\tilde{x}^T(PB + B^T P)\tilde{x} + \tilde{y}^T\tilde{u} - \tilde{x}^T P e_d \\ &\le -\tilde{x}^T(Q + kC^T C)\tilde{x} + \frac{1}{2}\tilde{x}^T PP^T\tilde{x} + \frac{1}{2}e_d^T e_d \\ &= -\tilde{x}^T(Q + kC^T C - \frac{1}{2}PP^T)\tilde{x} + \frac{1}{2}e_d^T e_d. \end{aligned} \tag{16}$$

Assuming that:

$$\begin{cases} kx_{2*}^2 > \frac{1}{2}L_0^2, \\ kx_{1*}^2 - \frac{C_0^2}{2} + R_0 - \frac{k^2 x_{1*}^2 x_{2*}^2}{kx_{2*}^2 - \frac{1}{2}L_0^2} > 0, \end{cases} \tag{17}$$

it is possible to obtain:

$$Q + kC^T C - \frac{1}{2}PP^T > 0. \tag{18}$$

Furthermore, it is possible to obtain:

$$\begin{aligned} \dot{W} \le -(1-\theta)\tilde{x}^T(Q + kC^T C - \frac{1}{2}PP^T)\tilde{x} + \theta\tilde{x}^T(Q + kC^T C \\ -\frac{1}{2}PP^T)\tilde{x} + \frac{1}{2}e_d^T e_d, \end{aligned}$$

where $0 < \theta < 1$ is a constant. Therefore, based on some algebraic manipulation, it is possible to obtain:

$$\dot{W} \le -(1-\theta)\tilde{x}^T(Q + kC^T C - \frac{1}{2}PP^T)\tilde{x}$$

for all:

$$\|\tilde{x}\| \ge \frac{\|e_d\|}{2\theta\lambda_{\min}(Q + kC^T C - \frac{1}{2}PP^T)},$$

with $\lambda_{\min}(\cdot)$ standing for the smallest eigenvalue of the corresponding matrix. Then, by utilizing Lemma 2, it can be shown that the map $\sum: e_d \to \tilde{x}$ is ISS.

This implies that $\tilde{x} = 0$ is a globally asymptotically stable equilibrium. In this way, the global tracking of trajectory (14) is achieved.

Remark 1*:* It is worth mentioning that from a practical point of view, condition (16) is reasonable. Obviously, it is noticed that this can be satisfied for the nominal circuit parameters of DC-DC boost converters in literatures such as [3], [4], [35] as long as *k* is properly chosen.

Remark 2: In the absence of various uncertainties, it is derived that:

$$\dot{\hat{d}}(t) = -\lambda\hat{d}(t),$$

which implies that $\hat{d}(t) \equiv 0$ if its initial value is chosen as $\hat{d}(0) = 0$. As for the proposed method, the control law is reduced to the controller in [32]. This means that the nominal performance of the proposed method is retained.

Remark 3: In the presence of circuit parameter perturbations, the obtained stability results are stricter when compared with [32]. A detailed analysis of this is shown in the Appendix.

IV. Simulation and Experimental Results

In this section, the control performances of the proposed method are validated by simulation and experimental studies. The passivity-based control (PBC), PID and PBC plus the extended state observer (ESO) methods are comparatively considered here to show the promising properties in terms of nominal performance recovery and disturbance rejection capability within the proposed PBC+GPIO approach.

A. PD Controller

Firstly, to underscore the limitations of a PD controller and the difficulties related to its tuning a local stability analysis of such a controller is presented. From system (1), without parameter perturbations, error dynamics are obtained:

$$\begin{aligned} L\dot{e}_1 &= -(1 - e_u - u_*)(e_2 + x_{2*}) + E, \\ C\dot{e}_2 &= (1 - e_u - u_*)(e_1 + x_{1*}) - \frac{e_2 + x_{2*}}{R}, \end{aligned} \tag{19}$$

where the errors are defined as:

$$e_1 = x_1 - x_{1*},\ e_2 = x_2 - x_{2*},\ e_u = u - u_*.$$

A standard PD controller for error dynamics (19) is given by:

$$e_u = k_p e_1 + k_d e_2,$$

where k_p, k_d are the tuning gains. Note that the computation of x_{1*} and the implementation of this controller require knowledge of *E*, *R*. A Jacobian matrix of the closed-loop system $\dot{e} = F(e)$, evaluated at the equilibrium point, is given by:

$$J = \begin{pmatrix} \nabla_{e_1}F_1(e) & \nabla_{e_2}F_1(e) \\ \nabla_{e_1}F_2(e) & \nabla_{e_2}F_2(e) \end{pmatrix}\Bigg|_{e=0} = \begin{pmatrix} \frac{k_p x_{2*}}{L} & \frac{-1 + u_* + k_d x_{2*}}{L} \\ \frac{1 - u_* - k_p x_{1*}}{C} & \frac{-1 - Rk_d x_{1*}}{RC} \end{pmatrix}.$$

Matrix *J* is a Hurwitz if and only if its trace is negative and its determinant is positive, which are given by:

$$\begin{aligned} tr(J) &= \frac{k_p x_{2*}}{L} - \frac{1 + Rk_d x_{1*}}{RC}, \\ \det(J) &= \frac{-k_p x_{2*} + R(u_* - 1)(u_* - 1 + k_p x_{1*} + k_d x_{2*})}{RLC}. \end{aligned}$$

The trace and determinant stability conditions can be written as the following two-side inequality:

$$\frac{k_p}{R(1-u_*)} + \frac{1 - u_* + k_p x_{1*}}{x_{2*}} > k_d > \frac{RCk_p x_{2*}}{Lx_{1*}} - \frac{1}{x_{1*}}, \tag{20}$$

TABLE I
PARAMETERS OF A DC-DC BOOST CONVERTER

Parameters	Symbols	Values
Input voltage	E_0	6 *V*
Desired output voltage	V_d	12 *V*
Inductance	L_0	10 *mH*
Capacitance	C_0	1000 *uF*
Load resistance	R_0	50 Ω
Parasitic resistance	r_L	1.7 Ω
Parasitic resistance	r_C	0.1 Ω

which is a conic section in the plane $k_p - k_d$. Inequality (19) reveals the conflicting role of the two gains. Notice that the circuit parameters (*L*, *C*, *R*, *E*) appear on both sides of the inequality. Therefore, it is difficult to select the optimal tuning gains of a conventional PID in the presence of time-varying disturbances. Moreover, the obtained stability result of the PID controller is local, while that of the proposed controller is global.

B. *Numerical Simulations*

The DC-DC boost converter is numerically simulated by using an average model in the presence of disturbances. The parameters in this test are shown in Table I. To achieve regulation of the output voltage, the control gain is chosen as k=0.025, which satisfies condition (16). In this particular case, the parameters of the GPI observers are taken as m=p=2, $\lambda_{10}=\omega_0^3$, $\lambda_{11}=3\omega_0^2$, $\lambda_{12}=3\omega_0$, $\lambda_{20}=\omega_1^3$, $\lambda_{21}=3\omega_1^2$, $\lambda_{22}=3\omega_1$, ω_0=100 and ω_1=200. For the PID controller, the gains are chosen as k_p = -0.5, k_I = -2 and k_d = -0.25. The initial values are selected as x_1 (0) = 5.5, x_2(0) = 0.05 and u(0) = 0.

1) Nominal Performance Recovery: A brief observation of Fig. 3 shows that the proposed control law results in the same transient responses as those of the baseline PBC method in the absence of disturbances, which verifies its nominal performance recovery property. However, it is shown that the conventional PID has a limited transient performance.

2) Load Resistance Disturbance Rejection: The robustness of the proposed controller against load resistance variations is examined. In the first simulation scenario, the step variation of the load resistance changing from 50Ω to 100Ω at t=0.5*sec* is considered. The response curves of the output voltage and inductor current under the baseline controller, PID, PBC+ESO and the proposed controller are provided in Fig.4. This figure shows that the baseline controller fails to remove the effects of the load resistance change. Although the output voltage offset is eliminated by means of adopting the PID and PBC+ESO, the maximum output voltage raises are 1.45*V* and 0.8*V*, respectively, which are larger than that of the proposed controller. Furthermore, the designed controller has a shorter

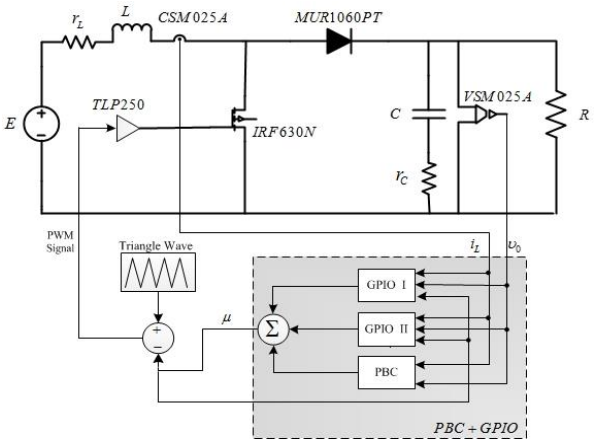

Fig. 2. Control system structure of a DC-DC boost converter.

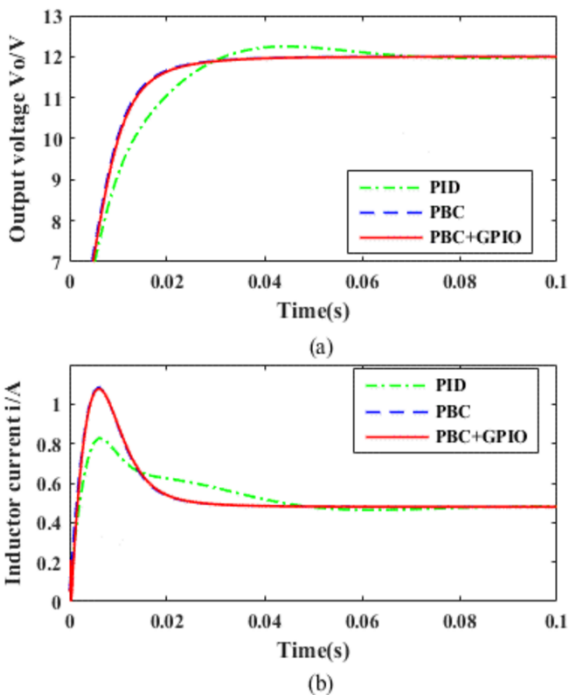

Fig. 3. Transient responses of a DC-DC boost converter under the PID (green line), PBC (blue line) and PBC+GPIO (red line) (simulation): (a) output voltage; (b) inductor current.

recovery time than those of the PID and PBC+ESO.

Then, like [33], a suitable output of the following nonlinear duffing chaotic system is considered as a model of the time varying load resistance:

$$\dot{\xi}_1 = \xi_2,$$
$$\dot{\xi}_2 = a\xi_1 - b\xi_1^3 - c\xi_2 + M\cos(2\pi f\tau),$$

where a = 1, b = 1, c = 1 and M = 1.

The time-varying load resistance is designed as $R(\tau)$=10ξ_1 (τ)+50. Fig. 6 shows that the PID and PID+ESO failed to remove the offset caused by the time-varying load resistance shown in Fig. 7, while the PBC+GPIO control law can effectively compensate this disturbance.

3) Input Voltage Disturbance Rejection: An input voltage disturbance of the step type is firstly considered for the DC-DC

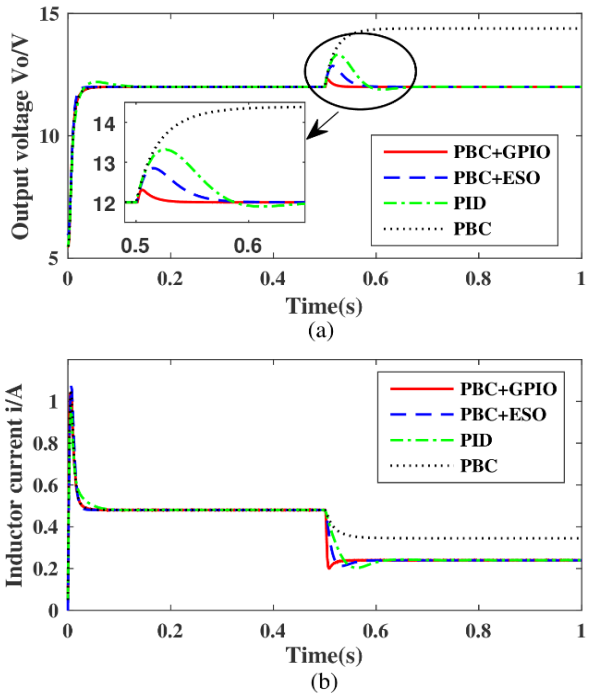

Fig. 4. Variable response curves of a DC-DC boost converter under the PBC+GPIO (red line), PBC+ESO (blue line), PID (green line) and PBC (black line) with a load resistance step variation (simulation): (a) output voltage; (b) inductor current.

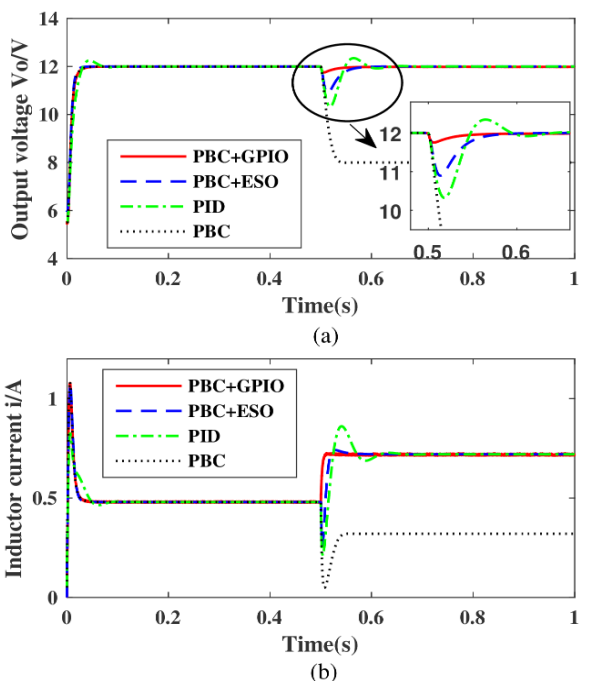

Fig. 5. Variable response curves of a DC-DC boost converter under the PBC+GPIO (red line), PBC+ESO (blue line), PID (green line) and PBC (black line) with an input voltage step variation (simulation): (a) output voltage; (b) inductor current.

boost converter. Response curves of the output voltage and inductor current of the boost converter under the PBC, PID, PBC+ESO and the designed controller are shown in Fig. 5.

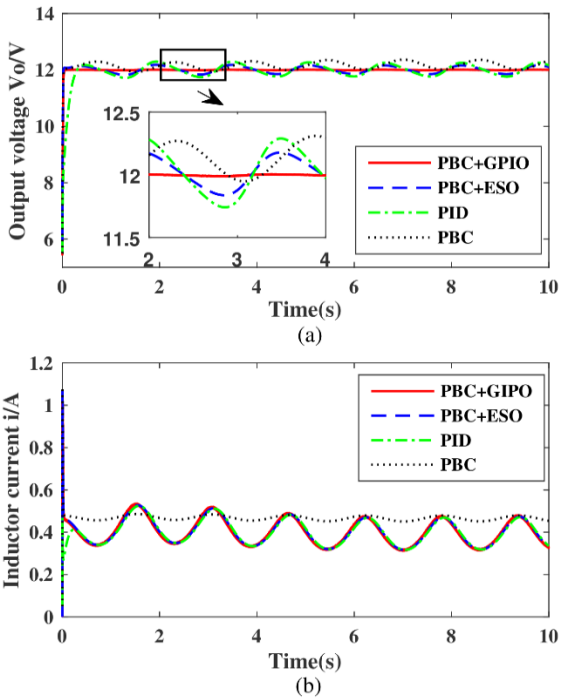

Fig. 6. Variable response curves of a DC-DC boost converter under the PBC+GPIO (red line), PBC+ESO (blue line), PID (green line) and PBC (black line) with a time-varying load resistance (simulation): (a) output voltage; (b) inductor current.

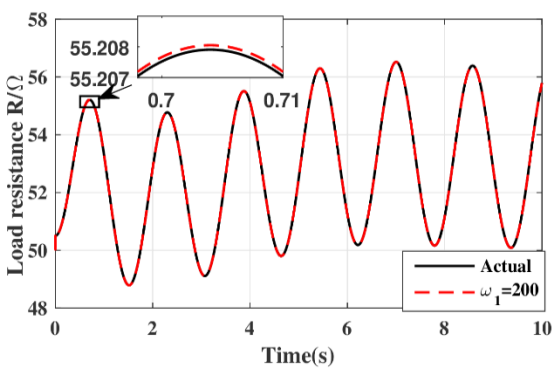

Fig. 7. Time-varying load resistance R (black line) and its estimation (red line) using *GPIO II* (simulation).

It is observed that proposed controller, PBC+ESO and PID control laws can eliminate the effect of input voltage changes. However, the presented control method obtains a better transient recovery performance. When the time-varying input voltage shown in Fig. 9 is applied to a DC-DC boost converter, it is clearly seen in Fig. 8 that the proposed controller rationally erase the offset. Finally, it is concluded that the designed controller outperforms the PBC+ESO and PID control methods in terms of anti-disturbance performance.

C. Experimental Results

Some experimental results are provided here to further examine the effectiveness of the proposed controller. A DC-DC boost prototype converter is built for the system shown

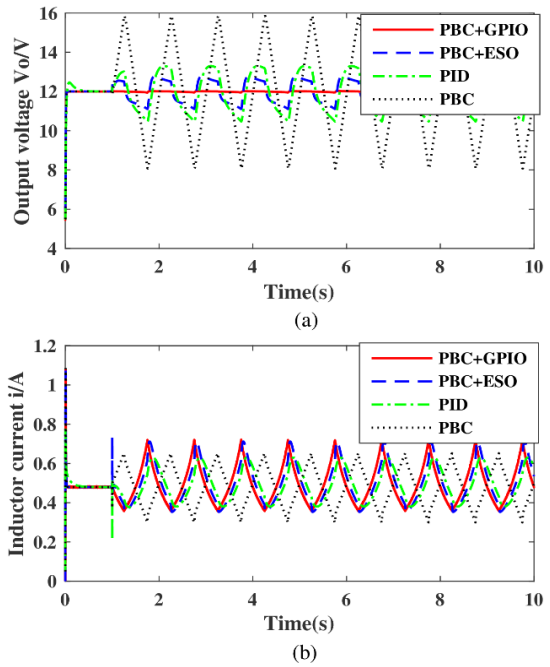

Fig. 8. Variable response curves of a DC-DC boost converter under the PBC+GPIO (red line), PBC+ESO (blue line), PID (green line) and PBC (black line) with a time-varying input voltage (simulation): (a) output voltage; (b) inductor current.

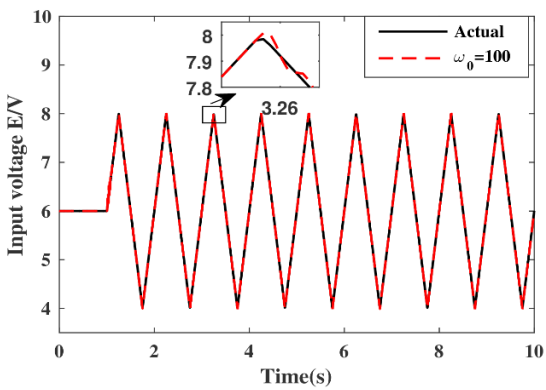

Fig. 9. Time-varying input voltage *E* (black line) and its estimation (red line) using *GPIO I* (simulation).

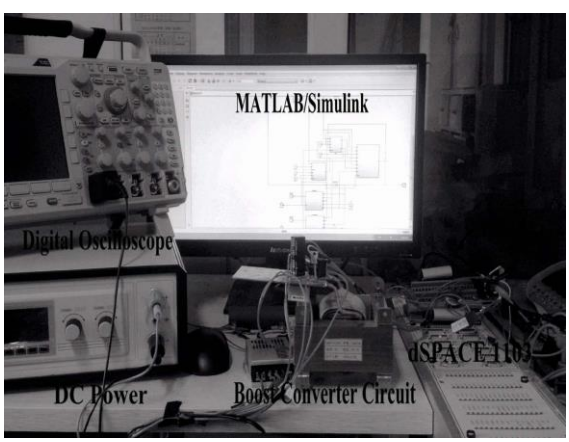

Fig. 10. Experimental setup system for a DC-DC boost converter.

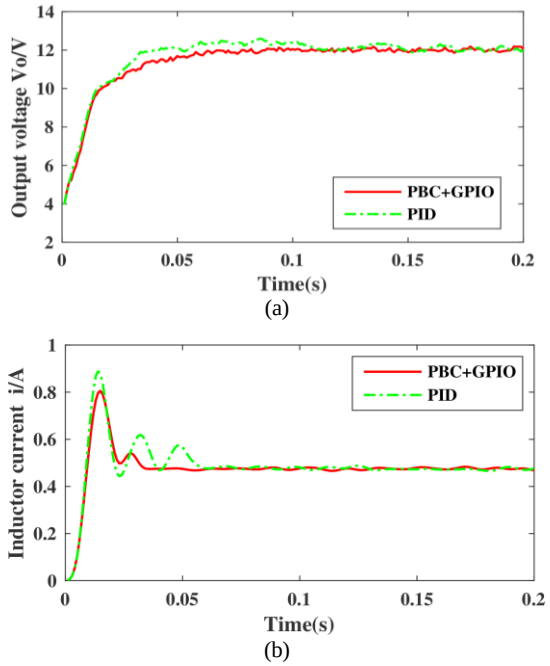

Fig. 11. Transient responses of a DC-DC boost converter under the PBC+GPIO (red line) and PID (green line) (experiment): (a) output voltage; (b) inductor current.

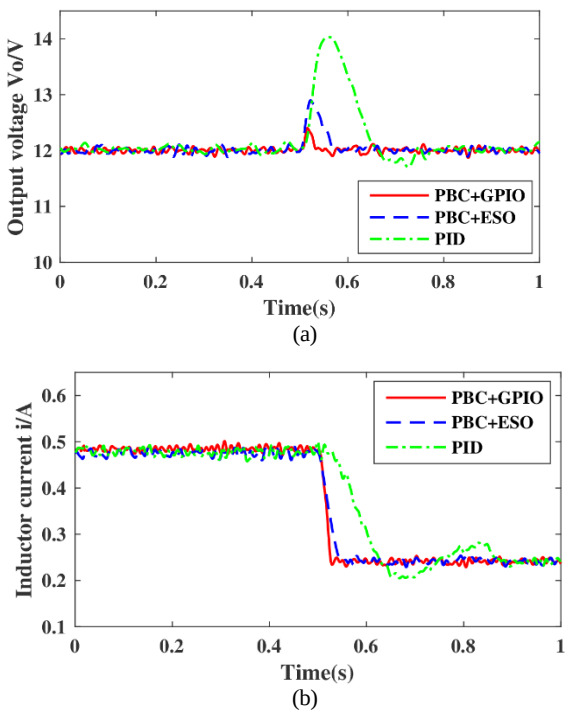

Fig. 12. Variable response curves of a DC-DC boost converter under the PBC+GPIO (red line), PBC+ESO (blue line) and PID (green line) with a load resistance step variation (experiment): (a) output voltage; (b) inductor current.

in Fig. 2 using a *MUR1060PT* diode and an *IRF630N* MOSFET driven by a *TLP250*. In addition, the inductor current and output voltage are measured by a *CSM025A* and a *VSM025A*, respectively, and converted though *A/D* converters. A photograph of the entire experimental setup is shown in Fig. 10.

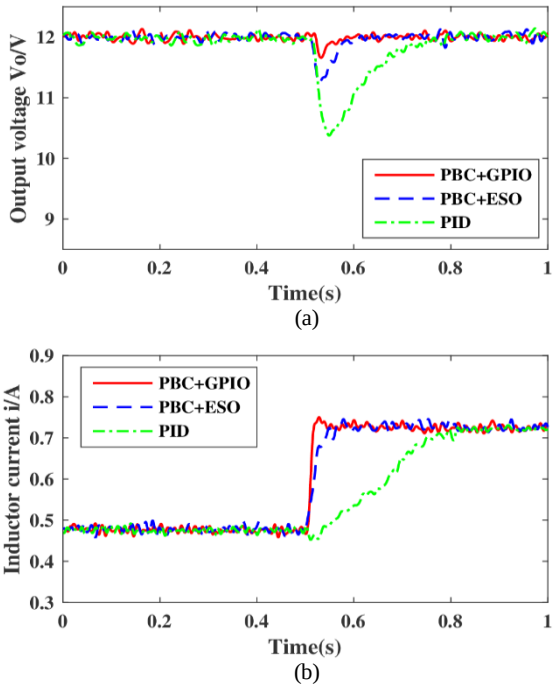

Fig. 13. Variable response curves of a DC-DC boost converter under the PBC+GPIO (red line), PBC+ESO (blue line) and PID (green line) with an input voltage step variation (experiment): (a) output voltage; (b) inductor current.

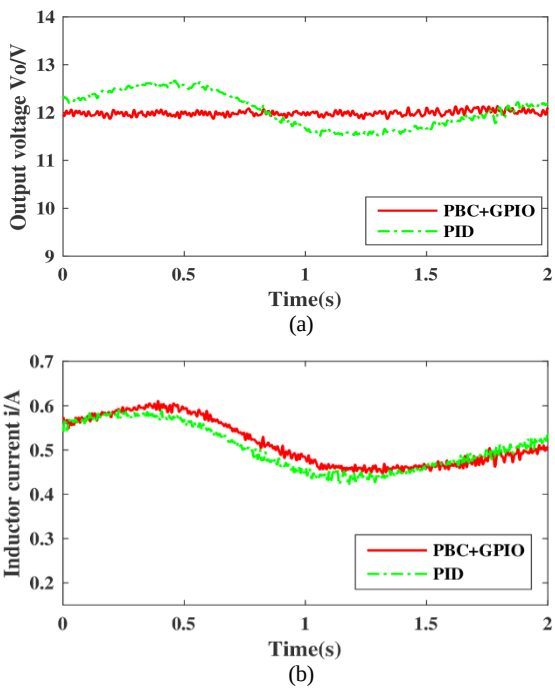

Fig. 14. Variable response curves of a DC-DC boost converter under the PBC+GPIO (red line) and PID (green line) with a time-varying load resistance (experiment): (a) output voltage; (b) inductor current.

For controlling the output voltage of the DC-DC boost converter, the PBC+GPIO is implemented by the MATLAB /Simulink program and a *dSPACE1103* microcontroller with a clock frequency of *100K Hz*. Actually, *dSPACE* was used to compile the *MATLAB*/ Simulink program into a C-program and then expedite the experimental work. In the *100%* hardware system, the whole control scheme can be implemented by a *DSP TMS320F240* with a clock frequency of *1MHZ*. The control algorithm is directly achieved using the C-program.

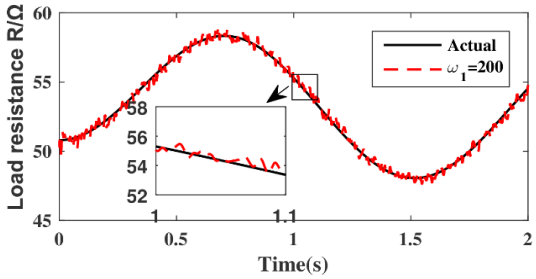

Fig. 15. Time-varying load resistance R (black line) and its estimation (red line) using *GPIO II* (experiment).

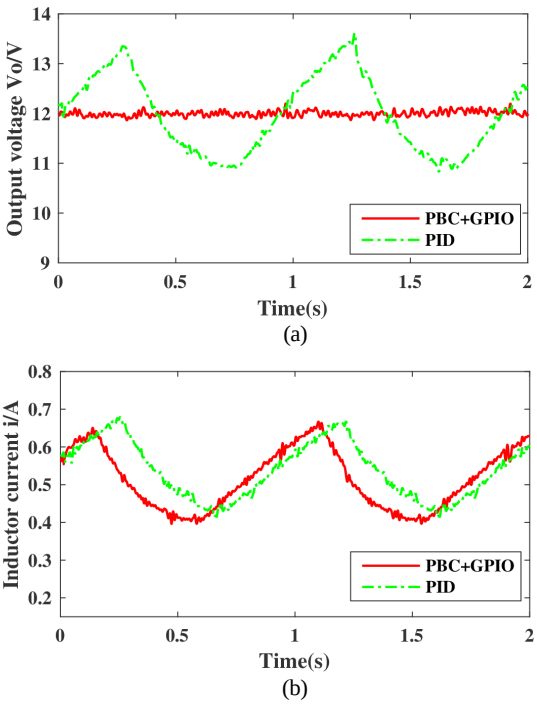

Fig. 16. Variable response curves of a DC-DC boost converter under the PBC+GPIO (red line) and PID (green line) with a time-varying input voltage (experiment): (a) output voltage; (b) inductor current.

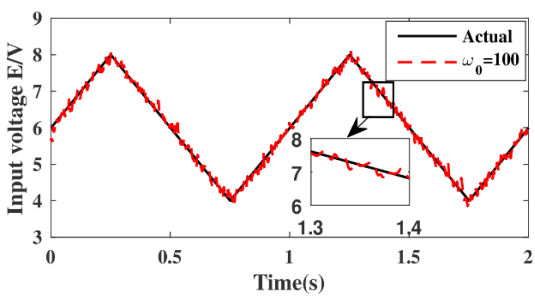

Fig. 17. Time-varying input voltage E (black line) and its estimation (red line) using *GPIO I* (experiment).

TABLE II
COMPARISON OF PERFORMANCE INDICES FOR ROBUSTNESS TESTS

Test Type	Controller	MOVD/R	RT	IAE
R: 50Ω→100Ω	PBC+GPIO	0.4V	0.0305s	0.0481
	PBC+ESO	0.9V	0.0629s	0.0795
	PID	2V	0.2198s	0.1105
E: 6 V → 4V	PBC+GPIO	0.3V	0.0635s	0.0584
	PBC+ESO	1.0V	0.0983s	0.0947
	PID	1.7V	0.2581s	0.1231

To validate the feasibility and effectiveness of the proposed approach, input voltage variations and load resistance changes are considered in the experimental cases.

In this set, comparison studies are carried out among the PID, the PBC+ESO and the proposed controller. The corresponding experimental results are shown in Figs. 11-17, where Fig. 11 shows that the designed controller has a better transient performance than that of the PID. It is clearly shown in Figs. 12-13 that the proposed approach has reasonably compensated the undesirable influences raised by disturbances of the step type with a better transient recovery and tracking performance. The detailed performance indices (including maximum output voltage drop/raise (MOVD/R), recovery time (RT), and the integral of the absolute error (IAE)) are provided in Table II. For time-varying disturbances, the PID and PBC+ESO methods, as in the simulations, have similar steady state performances. Therefore, a comparison study is carried out between the PID and the proposed controller. In the experimental studies the considered types of time-varying disturbances and their estimations are shown in Figs. 15 and 17. It is clearly observed in Figs. 14 and 16 that the PID controller fails to effectively reduce the influences of time-varying disturbances, while the proposed controller has a very nice control performance.

Overall, with respect to the PBC, PID, PBC+ESO, the proposed approach reveals a higher performance in the tracking and regulation modes and presents more robustness against time-varying disturbances in both the simulation and experimental studies.

V. CONCLUSIONS

In this paper, based on the passivity property and a GPI observer, a composite controller has been designed for DC-DC boost converters to achieve global tracking and robustness against uncertainties of various types. Both simulations and experimental studies have been provided to demonstrate the effectiveness as well as the superiorities of the proposed method. The results have shown that this approach reveals the properties of nominal performance recovery as well as good dynamic and static performances when compared with the PID and PBC+ESO methods.

APPENDIX

Detailed Analysis of Remark 3

To clearly explain Remark 3, the following analysis is given.

For a DC-DC boost converter, it is known that the internal circuit parameters, such as the inductance L or capacitances C, are usually varied by *20%*. Hence, it is possible to define:

$$L = L_0 + \Delta L,$$
$$C = C_0 + \Delta C,$$

where L_0, C_0 are the nominal values and $\Delta L, \Delta C$ are the perturbation terms. In [32], the authors failed to consider these parameter perturbations as lumped disturbances. Therefore, the dynamic model of a DC-DC boost converter is given as:

$$\dot{x} = \tilde{A}x + \tilde{u}B + \tilde{\eta}$$

where:

$$\tilde{A} = \begin{bmatrix} 0 & 0 \\ 0 & -\frac{1}{RC} \end{bmatrix}, \quad \tilde{B} = \begin{bmatrix} 0 & -\frac{1}{L} \\ \frac{1}{C} & 0 \end{bmatrix}, \quad \tilde{\eta} = \begin{bmatrix} E & 0 \end{bmatrix}^T.$$

It is seen that the system matrixes $\tilde{A}$ and $\tilde{B}$ always rely on the perturbation terms $\Delta L, \Delta C$. As stated in Assumption 1 of [32] and the problem formulation, a positive-definite symmetric matrix P should be found so that condition (4) is strictly satisfied. However, due to the fact that the exact values of $\Delta L, \Delta C$ are not known, it is only necessary to select:

$$P = \begin{bmatrix} L_0 & 0 \\ 0 & C_0 \end{bmatrix}.$$

Then the following is obtained:

$$\begin{aligned} P\tilde{B} + \tilde{B}^T P &= \begin{bmatrix} L_0 & 0 \\ 0 & C_0 \end{bmatrix} \begin{bmatrix} 0 & -\frac{1}{L_0 + \Delta L} \\ \frac{1}{C_0 + \Delta C} & 0 \end{bmatrix} \\ &\quad + \begin{bmatrix} 0 & \frac{1}{C_0 + \Delta C} \\ -\frac{1}{L_0 + \Delta L} & 0 \end{bmatrix} \begin{bmatrix} L_0 & 0 \\ 0 & C_0 \end{bmatrix} \\ &= \begin{bmatrix} 0 & -\frac{L_0}{L_0 + \Delta L} + \frac{C_0}{C_0 + \Delta C} \\ \frac{C_0}{C_0 + \Delta C} - \frac{L_0}{L_0 + \Delta L} & 0 \end{bmatrix} \\ &\neq 0. \end{aligned}$$

Hence, it is difficult to find a proper matrix P so that:

$$P\tilde{B} + \tilde{B}^T P \equiv 0, \tag{21}$$

which is an important condition for the stability analysis. It is clearly observed in Proposition 1 of [32] and (16) that if condition (21) is not strictly ensured, it is not possible to effectively eliminate the nonlinear term in the Lyapunov stability analysis. As a result, the stability result reported in [32]

is not rigorously ensured since it failed to consider the circuit parameter perturbations in the modeling process.

However, in this design, the circuit parameter perturbations are considered as the lumped disturbances d_1 and d_2 shown in (2) and (3). It is obvious that the system matrix B only depends on the nominal values L_0, C_0. It is not necessary to care if the influence of the parameter perturbations on the stability analysis holds since the two GPI observers have been designed to estimate the lumped disturbances d_1 and d_2 online.

Therefore, it is easy to find:

$$P = \begin{bmatrix} L_0 & 0 \\ 0 & C_0 \end{bmatrix}$$

so that:

$$PB + B^T P = \begin{bmatrix} L_0 & 0 \\ 0 & C_0 \end{bmatrix} \begin{bmatrix} 0 & -\frac{1}{L_0} \\ \frac{1}{C_0} & 0 \end{bmatrix} + \begin{bmatrix} 0 & \frac{1}{C_0} \\ -\frac{1}{L_0} & 0 \end{bmatrix} \begin{bmatrix} L_0 & 0 \\ 0 & C_0 \end{bmatrix}$$

$$= \begin{bmatrix} 0 & -\frac{L_0}{L_0} + \frac{C_0}{C_0} \\ \frac{C_0}{C_0} - \frac{L_0}{L_0} & 0 \end{bmatrix} = \begin{bmatrix} 0 & -1+1 \\ 1-1 & 0 \end{bmatrix} \equiv 0.$$

Finally, as presented in Proposition 1, the global asymptotic stability of the overall system is strictly ensured even in the face of the time-varying parameter perturbations. Compared with [32], the stability results in this paper are stricter.

ACKNOWLEDGMENT

This work is supported by National Natural Science Foundation of China (61473080, 61573099), 333 Talents Program of Jiangsu Province and Fundamental Research Funds for the Central Universities and Graduate Innovation Program in Jiangsu Province (KYLX15-0115).

REFERENCES

[1] L. S. Yang and C. C. Lin, "Analysis and implementation of a DC-DC converter for hybrid power supplies systems," *J. Power Electron.*, Vol. 15, No. 6, pp. 1438-1445, Nov. 2015.

[2] M. Pahlevaninezhad, P. Das, J. Drobnik, P. K. Jain, and A. Bakhshai, "A ZVS interleaved boost AC-DC converter used in plug-in electric vehicles," *IEEE Trans. Power Electron.*, Vol. 27, No. 8, pp. 3513-3529, Aug. 2012.

[3] Y. X. Wang, D. H. Yu, and Y. B. Kim, "Robust time-delay control for the DC-DC boost converter," *IEEE Trans. Ind. Electron.*, Vol. 61, No. 9, pp. 4829-4837, Sept. 2014.

[4] P. Karamanakos, T. Geyer, and S. Manias, "Direct voltage control of DC-DC boost converters using enumeration-based model predictive control," *IEEE Trans. Power Electron.*, Vol. 29, No. 2, pp. 968-978, Feb. 2014.

[5] R. Ortega, G. Espinosa-Perez, and A. Astolfi, "Passivity-based control of AC drives: theory for the user and application examples," *International Journal of Control*, Vol. 86, No. 4, pp. 625-635, Jan. 2013.

[6] Q. L. Tong, Q. Zhang, R. Min, X. C. Zou, Z. L. Liu, and Z. Q. Chen, "Sensorless predictive peak current control for boost converter using comprehensive compensation strategy," *IEEE Trans. Ind. Electron.*, Vol. 61, No. 6, pp. 2754-2766, Jun. 2014.

[7] L. Martinez-Salamero, G. Garcia, M. Orellana, C. Lahore, and B. Estibals, "Start-up control and voltage regulation in a boost converter under sliding-mode operation," *IEEE Trans. Ind. Electron.*, Vol. 60, No. 10, pp. 4637-4649, Oct. 2013.

[8] S. M. Chen, T. J. Liang, L. S. Yang, and J. F. Chen, "A cascaded high step-up DC-DC converter with single switch for microsource applications," *IEEE Trans. Power Electron.*, Vol. 26, No. 4, pp. 1146-1153, Apr. 2011.

[9] H. El-Fadil, F. Giri, O. El-Magueri, and F. Z. Chaoui, "Control of DC-DC power converters in the presence of coil magnetic saturation," *Control Engineering Practice*, Vol. 17, No. 7, pp. 849-862, Jul. 2009.

[10] C. Olalla, R. Leyva, A. El-Aroudi, P. Garces, and I. Queinnec, "LMI robust control design for boost PWM converters," *IET Power Electron.*, Vol. 3, No. 1, pp. 75-85, Jan. 2010.

[11] C. L. Zhang, J. X. Wang, S. H. Li, B. Wu, and C. J. Qian, "Robust control for PWM-based DC–DC buck power converters with uncertainty via sampled-data output feedback," *IEEE Trans. Power Electron.*, Vol. 30, No. 1, pp. 504-515, Jan. 2015.

[12] I. Yazici, "Robust voltage mode controller for DC-DC boost converter," *IET Power Electron.*, Vol. 8, No. 3, pp. 342-349, Mar. 2014.

[13] J. X. Wang, S. H. Li, J. Yang, B. Wu, and Q. Li, " Extended state observer based sliding mode control for PWM-based DC–DC buck power converter systems with mismatched disturbances," *IET Power Electr*on., Vol. 9, No. 4, pp. 579-586, Feb. 2015.

[14] M. Salimi and A. Zakipour, "Lyapunov based adaptive robust control of the non-minimum phase DC–DC converters using input–output linearization," *J. Power Electron.*, Vol. 15, No. 6, pp. 1577-1583, Nov. 2015.

[15] H. X. Liu and S. H. Li, "Speed control for PMSM servo system using predictive functional control and extended state observer," *IEEE Trans. Ind. Electr*on., Vol. 59, No. 2, pp. 1171-1183, Feb. 2012.

[16] V. Utkin, "Sliding mode control of DC-DC converters," *Journal of the Franklin Institute*, Vol. 350, No. 8, pp. 2146-2165, Oct. 2013.

[17] C. Olalla, I. Queinnec, R. Leyva, and A. EI-Aroundi, "Robust optimal control of bilinear DC-DC converters," *Control Engineering Practice*, Vol. 19, No. 7, pp. 688-699, Jul. 2011.

[18] P. Sun and L. Zhou, "Duty ratio predictive control scheme for digital control of DC-DC switching converters," *J. Power Electron.*, Vol. 11, No. 2, pp. 315-320, Mar. 2006.

[19] C. Chang, Y. Yuan, T. Jiang, and Z. Zhou, "Field programmable gate array implementation of a single-input fuzzy proportional–integral–derivative controller for DC–DC buck converters," *IET Power Electr*on., Vol. 9, No. 6, pp. 1259-1266, Apr. 2016.

[20] R. J. Wai and L. C. Shi, "Adaptive fuzzy-neural-network design for voltage tracking control of a DC-DC boost converter," *IEEE Trans. Power Electron.*, Vol. 27, No. 4, pp. 2104-2115, Apr. 2012.

[21] S. R. Sanders and G. C. Verghese, "Lyapunov-based control for switched power converters," *IEEE Trans. Power Electron.*, Vol. 7, No. 1, pp. 17-24, Jan. 1992.

[22] S. H. Li and Z. G. Liu, "Adaptive speed control for permanent magnet synchronous motor system with variations of load inertia," *IEEE Trans. Ind. Electron.*, Vol. 56, No. 8, pp. 3050-3059, Aug. 2009.
[23] R. Ortega, J. A. L. Perez, P. J. Nicklasson, and H. Sira-Ramirez, *Passivity-based Control of Euler-Lagrange Systems: Mechanical, Electrical and Electromechanical Applications*, Series Comunications and Control Engineering, chap. 3, pp. 428-640, 1998.
[24] R. Ortega, A. J. Van der Schaft, I. Mareels, and B. M. Maschke, "Putting energy back in control," *IEEE Contr. Syst. Mag.*, Vol. 21, No. 2, pp. 18-33, Apr. 2001.
[25] F. Doerfler, J. K. Johnsen, and F. Allgoewer, "An introduction to interconnection and damping assignment passivity based control in process engineering," *J. Process Contr.*, Vol. 19, No. 9, pp. 1413-1426, Oct. 2009.
[26] A. J. Van der Schaft, *L_2-gain and Passivity Techniques in Nonlinear Control*, Springer, 1996.
[27] A. Y. Achour, B. Mendil, S. Bacha, and I. Munteanu, "Passivity-based current controller design for a permanent-magnet synchronous motor," *ISA Transactions*, Vol. 48, No. 3, pp. 336-346, Jul. 2009.
[28] H. K. Khalil, *Nonlinear Systems*, 2nd ed., Prentice-Hall, 1996.
[29] C. Ren and S. Ma, "Generalized proportional integral observer based control of an omnidirectional mobile robot," *Mechatronics*, Vol. 26, pp. 36-44, Mar. 2015.
[30] C. Y. Chan, "Simplified parallel-damped passivity based controllers for DC-DC power converters," *Automatica*, Vol. 44, No. 11, pp. 2977-2980, Nov. 2008.
[31] S. H. Li, J. Yang, W. H. Chen, and X. S. Chen, *Disturbance Observer-based Control: Methods and Applications*, CRC press, 2014.
[32] R. Cisneros, M. Pirro, G. Bergna, R. Ortega, G. Ippoliti, and M. Molinas, "Global tracking passivity-based PI control of bilinear systems: application to the interleaved boost and modular multilevel converters," *Control Engineering Practice*, Vol. 43, pp. 109-119, Oct. 2015.
[33] A. Hernandez-Mendez, J. Linares-Flores, and H. Sira-Ramirez, "A backstepping approach to decentralized active disturbance rejection control of interacting boost converters," *IEEE Trans. Ind. Appl.*, Vol. 53, No. 4, pp. 4063-4072, Jul./Aug. 2017.
[34] Y. I. Son and I. H. Kim, "Complementary PID controller to passivity-based nonlinear control of boost converters with inductor resistance," *IEEE Trans. Contr. Syst. Technol.*, Vol. 20, No. 3, pp. 826-834, May 2012.
[35] J. Linares-Flores, A. Hernandez-Mendez, C. Garcia-Rodriguez, and H. Sira-Ramirez, "Robust nonlinear adaptive control of a "boost" converter via algebraic parameter identification," *IEEE Trans. Ind. Electron.*, Vol. 61, No. 8, pp. 4105-4114, Aug. 2014.
[36] R. J. Wai and L. C. Shih, "Design of voltage tracking control for DC-DC boost converter via total sliding-mode technique," *IEEE Trans. Ind. Electron.*, Vol. 58, No. 6, pp. 2502-2511, Jun. 2011.
[37] M. Hernandez-Gomez, R. Ortega, F. Lamnabhi-Lagarrigue, and G. Escobar, "Adaptive PI stabilization of switched power converters," *IEEE Trans. Contr. Syst. Technol.*, Vol. 18, No. 3, pp. 688-698, May 2010.
[38] J. Q. Han, "From PID to active disturbance rejection control," *IEEE Trans. Ind. Electron.*, Vol. 56, No. 3, pp. 900-906, Mar. 2009.
[39] J. X. Wang, C. L. Zhang, S. H. Li, J. Yang, and Q. Li, "Finite-time output feedback control for PWM-based DC-DC buck power converters of current sensorless mode," *IEEE Trans. Contr. Syst. Technol.*, Vol. 25, No. 4, pp. 1359-1371, Jul. 2017.

Wei He was born in Fukang, Xinjiang Province, China. He received his B.S. degree from the Shenyang University of Chemical Technology, Shenyang, China, in 2010; and his M.S. from the Shenyang University of Technology, Shenyang, China, in 2014. He is presently working towards his Ph.D. degree in the School of Automation, Southeast University, Nanjing, China. His current research interests include nonlinear control, passivity based control and disturbance rejection with application to power electronic systems.

Shihua Li was born in Pingxiang, Jiangxi Province, China, in 1975. He received his B.S., M.S. and Ph.D. degrees all in Automatic Control from Southeast University, Nanjing, China, in 1995, 1998 and 2001, respectively. Since 2001, he has been with the School of Automation, Southeast University, where he is presently working as a Professor and as the Director of the Mechatronic Systems Control Laboratory. His current research interests include modeling, analysis and nonlinear control theory (non-smooth control, disturbance rejection control, adaptive control, etc.) with application to mechatronic systems, including manipulators, robots, AC motors, power electronic systems and so on. He has authored or coauthored over 200 technical papers and two books in these areas. He is a Member of the Technical Committee on System Identification and Adaptive Control of the IEEE CSS and a Member of the Electrical Machines Technical Committee and Motion Control Technical Committee of the IEEE IES. He is serving as an Associate Editor or Editor of the International Journal of Robust and Nonlinear Control, IET Power Electronics and International Journal of Electronics. He is also a Guest Editor of the IEEE Transactions on Industrial Electronics, International Journal of Robust and Nonlinear Control and IET Control Theory and Applications. He is the Vice Chairman of the IEEE CSS Nanjing Chapter.

Jun Yang was born in Anlu, Hubei Province, China, in 1984. He received his B.S. degree from the Department of Automatic Control, Northeastern University, Shenyang, China, in 2006; and his Ph.D. degree in Control Theory and Control Engineering from the School of Automation, Southeast University, Nanjing, China, where he is presently working as an Associate Professor. His current research interests include disturbance estimation and compensation, advanced control theory and its application to flight control systems and motion control systems. He is serving as an Associate Editor of the Transactions of the Institute of Measurement and Control.

Zuo Wang was born in Xuzhou, Jiangsu Province, China. He received his B.S. degree from Hohai University, Nanjing, China, in 2013. He is presently working towards his Ph.D. degree in the School of Automation, Southeast University, Nanjing, China. His current research interests include the design and implementation of advanced control strategies with application to power converters.